

LEARNING SHAPE STATISTICS FOR HIERARCHICAL 3D MEDICAL IMAGE SEGMENTATION

Wuxia Zhang, Yuan Yuan, Xuelong Li, Pingkun Yan

Center for OPTical IMagery Analysis and Learning (OPTIMAL), State Key Laboratory of Transient Optics and Photonics, Xi'an Institute of Optics and Precision Mechanics, Chinese Academy of Sciences, Xi'an 710119, Shaanxi, P. R. China

ABSTRACT

Accurate image segmentation is important for many medical imaging applications, whereas it remains challenging due to the complexity in medical images, such as the complex shapes and varied neighbor structures. This paper proposes a new hierarchical 3D image segmentation method based on patient-specific shape prior and surface patch shape statistics (SURPASS) model. In the segmentation process, a coarse-to-fine, two-stage strategy is designed, which contains global segmentation and local segmentation. In the global segmentation stage, patient-specific shape prior is estimated by using manifold learning techniques to achieve the overall segmentation. In the second stage, SURPASS is computed to solve the problem of poor segmentation at certain surface patches. The effectiveness of the proposed 3D image segmentation method has been demonstrated by the experiments on segmenting the prostate from a series of MR images.

Index Terms— 3D image segmentation, shape modeling, manifold learning, surface patch shape statistics

1. INTRODUCTION

Segmenting anatomical structures from 2D or 3D medical images with accuracy is an important processing step in a wide range of applications. In the recent years, shape prior based deformable models such as active shape model (ASM) [1] have been shown to be successful in medical image segmentation.

Extending the ASM methodology to 3D space is an intuitive procedure to be considered. Many studies have focused on building statistical models from 3D training data sets [2, 3]. Most of these developments, which are true for dense 3D data sets, have focused on landmark generation, statistical shape model and deformable model.

Multi-slice image data is routinely obtained in the clinical practice. Due to the large inter-slice distance, it is difficult to extract 3D targets directly from multi-slice data sets. Therefore, slices in those data sets are inclined to be segmented as separated 2D images. In light of the above, Zhu *et al.* [4] proposed a hybrid ASM approach. The essential idea of Zhu's

work contains two aspects. First, the 2D deformable model is performed on each slice to get 2D optimization on individual slices. Second, for the sake of obtaining the anatomical boundary of the complete 3D target, the 3D shapes can be constructed from 2D contours using a 3D shape model. In Zhu's work, the 3D shape model is constructed via principal component analysis (PCA), which is suitable to model linear variation. However, in many real-world medical segmentation problems, the subspace of the data set is nonlinear. Nonlinear subspace represented by linear methods like PCA may not make sense, since some important information can be lost. This problem may largely influence the accuracy of shape prior estimation. We propose a novel method to estimate patient-specific shape priors to achieve more accurate segmentation by using manifold learning.

Another problem in 3D medical image segmentation is that the optimal segmentation results in the large are frequently poor at several surface patches by using one single model [6]. Thus, we present to segment an image using surface patch shape statistics (SURPASS) to achieve more accurate segmentation at each local patch. For the purpose of assuring anatomical shape in the valid range, we propose a new method of leaning SURPASS and use it for segmentation.

The rest of the paper is organized as follows. In section 2, the method of hierarchical segmentation is presented. In section 3, global segmentation is provided. In section 4, the local segmentation is described in detail. In section 5, a series of experiments are conducted to validate the performance of the proposed method. The paper is concluded in Section 6.

2. HIERARCHICAL SEGMENTATION

Our proposed hierarchical segmentation method is shown in Fig. 1. In the phase of global segmentation, the complete 2D deformable model based segmentation is performed on all slices. During each iteration, the previous segmentation result is first projected into the same manifold with the training shapes. The shape prior is then estimated through the nearest-neighbor graph. Under the guidance of 3D shape prior that is

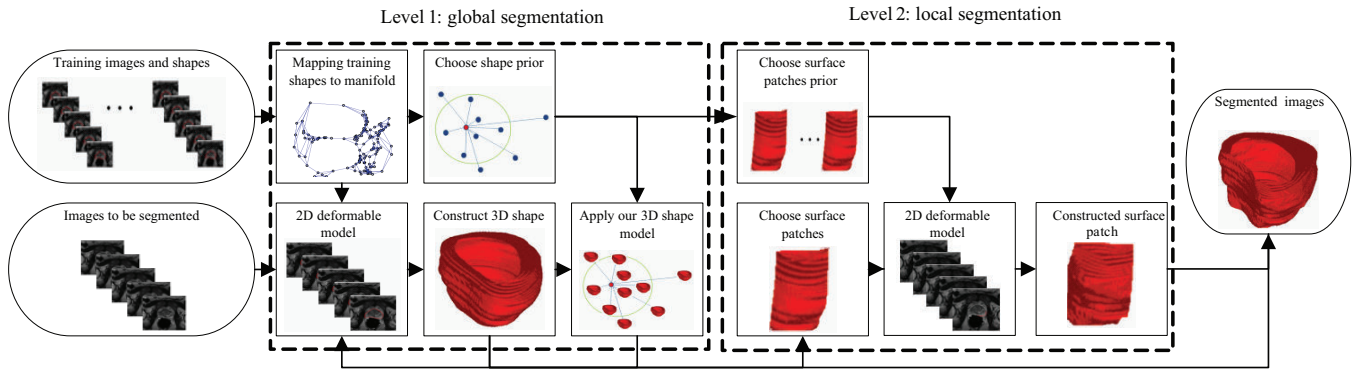


Fig. 1. Flow chart of the proposed method.

seen as initialization of 2D shape instance, 2D deformable model is employed to segment a series of MR images of the patient for extracting surfaces. The above-mentioned steps will be repeated until a satisfactory result is obtained. In the phase of local segmentation, local segmentation aims to re-segment the surface patches of poor segmentation in order to further improve the accuracy. The surfaces are divided into patches according to a specified scheme. The patches with large deformation are chosen for both training surfaces and global segmenting surface. It will be explained in detail in Section 4. Then, the 2D deformable model is employed on the segment of each slice for extracting patches. The patches segmented poorly in the first level are replaced by refined patches in the second level, which results in the ultimate segmentation.

3. GLOBAL SEGMENTATION

3.1. Estimating patient-specific shape prior

During the segmentation process, the shape prior of an object can be estimated by using shape statistics according to training shapes. If the whole training shapes are used for shape estimation, “blurred” shape prior may be estimated, which is far away from the desirable segmentation result. In order to address the problem, only training shapes which are similar to patient-specific shape will be used for shape estimation. Therefore, a new method is proposed in our paper.

In our work, a shape is described by n landmark points $(x_1, y_1) \cdots (x_n, y_n)$ forming a shape vector $S = (x_1, y_1, \cdots, x_n, y_n)^T$. The landmark points are obtained by sampling the contour equally Euclidean distance spaced. Each $2n$ dimensional shape vector is then mapped to m dimensional manifold for shape learning and prior estimation, where $m \ll 2n$.

In order to obtain the patient-specific prior, we propose a method based manifold learning. In this paper, Isometric Feature Mapping (ISOMAP) algorithm [5] is used. We give a description of how to get patient-specific shape prior as follows.

- Project the learning set $\{S_i\}$ into a feature subspace via ISOMAP algorithm.
- Construct the adjacent graph. The i th vertex s_i corresponds to the shape S_i in the original shape space. Find the geodesics (=shortest paths on the graph) between all pairs of vertices by Dijkstra’s algorithm.

$$d_{ij} = \arg \min_j \sum_i g(s_i, s_j) \quad (1)$$

where g is the length of the shortest path, s_i and s_j denote the corresponding shape after manifold.

- Construct the nearest-neighbor graph by connecting k -Nearest Neighbor (k NN) for each shape based on the edge lengths. The constructed nearest-neighbor graph is an approximation of the local manifold structure.
- Compute weight.

$$w_j^{(i)} = e^{-\frac{d_{ij}}{\sigma}}, \quad (2)$$

where σ is a suitable constant. d_{ij} denotes the geodesics distance between s_i and s_j .

- Construct patient-specific shape prior. The shape in the high-dimensional space is computed using appropriate high-dimensional features of the k nearest neighbors and the reconstructed weights [7].

$$\hat{S}_i = \sum_{j=1}^k w_j^{(i)} S_{N(j)}, \quad (3)$$

where \hat{S}_i can be linearly reconstructed in terms of its neighbors $S_{N(1)}, \cdots, S_{N(k)}$ with corresponding weight $w_j^{(i)}$. Since the weight $w_j^{(i)}$ is the similarity measure between S_i and its neighbors $S_{N(1)}, \cdots, S_{N(k)}$, the obtained shape is patient-specific. After experimenting with different values of k , 6 is chosen in our study, which gave the best result in our experiments.

3.2. Global deformation

Similar to ASM [1], the deformable model has two terms in its energy functional

$$E = E_{image} + E_{shape}. \quad (4)$$

The segmentation is achieved by minimizing the above energy in an iterative way. Each iteration contains two steps to minimize the image energy and shape energy terms, respectively. The two steps are described in detail as follows.

- Image energy minimization
 1. Examine a region of the image around each landmark point S_i to find the best nearby match for the point S'_i .
 2. Update the parameters (X_t, Y_t, s, θ) to best fit the new found points S .

In practice, we look along the normal directions of the contour at each landmark point to find the object boundary. S is a shape vector containing n landmark points. The parameters (X_t, Y_t, s, θ) represent x -axis shift (right), y -axis shift (down), scale, rotation. The parameters are set by the user.

- Shape energy minimization
 1. Map the current contour S_i obtained at the i th iteration to the same manifold space with the training shapes. The projected shape is denoted by \hat{s}_i .
 2. Compute the geodesic distance between each training shape and \hat{s}_i .
 3. Select training shapes according to \hat{s}_i using k NN algorithm on the adjacent graph.
 4. Project the step 3 result onto the original space and apply equation (3) to achieve \hat{S}_i .

In our work, the segmentation is initialized by using the mean shape computed from the training shapes.

4. LOCAL SEGMENTATION

The number of surface patch should be set appropriately. If excessively small, the patch is too large to preserving subtle information, because local information available is not adequate for local shape training. If extremely large, the patch is too small to keep the surface smooth. After experimenting with different number, we manually set a division scheme for dividing the surface mesh into eight sub-regions which balance the above two extreme cases. These patches overlap with eight points on each slice in order to maintain deformation continuity on the surface. Statistical analysis is employed to deal with the AMD error and the result is show in Fig.2 (a). It can be seen that some surface patches like 5, 6, 7 and 8 are poor segmented, whereas the segmentation of other patches is relatively accurate. The patches of poor segmentation show large deformation (great curvature) visually in Fig.2 (b). With the aim of making further accuracy of segmentation, it is natural to re-segment the surface patch of poor segmentation. We propose to learn SURPASS to refine image segmentation.

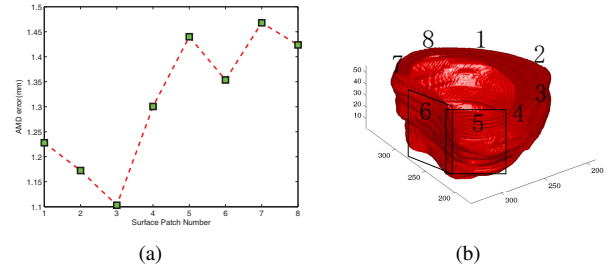


Fig. 2. the AMD error represents average minimum distance between the surface patch of 10 patients and corresponding surface patch of the ground truth in Fig.2 (a). Surface patches division is shown in Fig.2 (b).

4.1. Learning SURPASS and local deformation

Local information is used to guide region segmentation [8]. We proposed the concept of SURPASS, for SURPASS exhibits the superiority of processing image patches for its elastic properties. For incorporating more subtle prior information, Learning SURPASS can segment more precisely.

According to the mean shape of the training set, the surface patches with large deformation (great curvature) are selected. The patch segmentation is initialized by the average of training segments. Owing to the segment of low dimension, we apply eigenvalue decomposition to shape model instead of PCA or manifold learning. The subtle information is completely preserved via the above means. That is the reason why Learning SURPASS method is able to receive much better segmentation of patches.

The local deformation strategy is almost the same as the global deformation strategy. Subsequently, the 2D deformable model is performed on each slice to find the best segment. Then, we updated the new segmentation result of the surface patches to the global segmentation result.

5. EXPERIMENTS

5.1. Data

The experiment data consists of 10 prostate gland MRI sequences, totaling 260 slices. Each slice contains 512×512 pixels, with the pixel size of $0.3\text{mm} \times 0.3\text{mm}$. Each slice is 3mm thick and has 0.5mm interslice gap. All the images were annotated by an expert radiologist, which were considered as gold standard for validation. The contour of each slice is represented by 64 landmarks. The number of slices with manual segmentation is different for patients. It is shown in Table 1, where PN represents the patient number, SN denotes the number of slices with manual segmentation. For the purpose of assuring the data for each patient with the same dimension, a series of preprocessing steps are performed. First, 15 dimension is selected based on the principle of preserving the most ground truth. Second, larger than 15, slices are extracted; less than 15, slices are interpolated according to the

similarity measure respectively.

Table 1. the different number of slices with manual delineation for different patients.

PN	1	2	3	4	5	6	7	8	9	10
SN	11	15	13	13	16	18	10	16	15	13

5.2. Results

As the number of the sample was relatively limited, cross validation with leave-one-out strategy was applied to investigate the performance of the developed approach. Our method was implemented using Matlab. The computation time for segmenting one patient data is around 120s on a 3.0 GHz Intel PC with 2GB RAM.

Fig. 3 presents a series of examples of the 3D prostate segmented using both our developed method and Zhu’s method [4] together with the ground truth, for visual comparison. It can be seen that segmentation based on our proposed method is much better than segmentation based on the Zhu’s method and visually as good as manual segmentation. The performance of our proposed method was quantitatively evaluated by the average surface distance between the automatic segmentation and the manual segmentation. The segmentation results of Zhu’s method are also included for comparison. The evaluation results are given in Table 2. It can be seen that the average surface distances for global method and our method are about 4.68 pixels (1.40mm) and 3.82 pixels (1.15mm) respectively, compared to 6.98 pixels (2.09mm) for Zhu’s method.

Table 2. Average surface distance between the manual segmentation and the automated segmentation of 10 patients.

method	metric	mean±std	min	median	max
zhu’s method	pixel	6.98±1.97	3.62	7.63	9.04
	mm	2.09±0.59	1.09	2.29	2.71
global method	pixel	4.68±1.39	2.94	4.61	8.02
	mm	1.40±0.42	0.88	1.38	2.41
our method	pixel	3.82±1.19	2.43	3.65	6.77
	mm	1.15±0.36	0.73	1.1	2.03

6. CONCLUSION

In this paper, we propose a novel hierarchical strategy to solve two difficult cases in 3D MRI segmentation. Estimating patient-specific shape prior is used to address “blurred” shape prior by manifold learning. We present the Learning SURPASS to address another difficulty of poor segmentation at certain surface patches. It has been shown that our proposed algorithm can outline the prostate surface from a series of MR images more accurately, compared to other state-of-the-art methods.

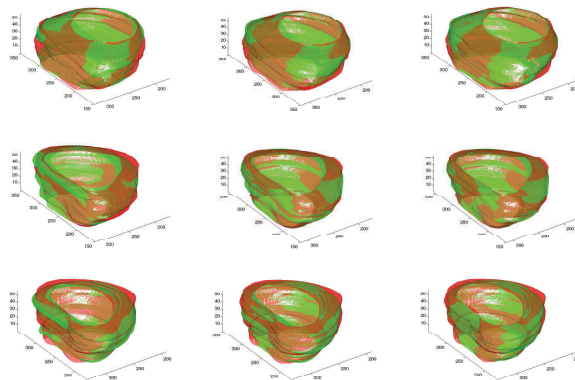


Fig. 3. Segmentation results of Zhu’s method (left column), our global method (middle column) and our proposed method (right column) are shown, together with the corresponding manual segmentation. The red surfaces represent ground truth and the green surfaces visualize the automatic segmentation results obtained using different methods.

7. ACKNOWLEDGEMENTS

The presented research work is supported by the National Basic Research Program of China (973 Program) (Grant No. 2011CB707000), the National Natural Science Foundation of China (Grant No. 61072093) and the Open Project Program of the State Key Lab of CAD & CG (Grant No. A1116), Zhejiang University.

8. REFERENCES

- [1] T. F. Cootes, C. J. Taylor, D. H. Cooper, and J. Graham, “Active shape models - their training and application,” *Computer Vision and Image Understanding*, vol. 61, no. 1, pp. 38-59, 1995.
- [2] R. H. Davies, C. J. Twining, T. F. Cootes, and C. J. Taylor, “Building 3-D Statistical Shape Models by Direct Optimization,” *IEEE Trans. Medical Imaging*, vol.29, pp. 961-981, 2010.
- [3] Y. Wang, H. N. Cardinal, D. B. Downey and A. Fenster, “Semi-automatic three-dimensional segmentation of the prostate using two-dimensional ultrasound images,” *Medical Physics*, vol. 30, pp.887-897, 2003.
- [4] Y. Zhu, S. Williams, and R. Zwigelaar, “A Hybrid ASM Approach for Sparse Volumetric Data Segmentation,” *Pattern Recognition and Image Analysis*, vol. 17, pp. 252-258, 2007.
- [5] small P. Etyngier, Ségonne and R. Kwriwen, “Shape Prior using Manifold Learning Techniques,” in *Proc. IEEE International Conference on Computer Vision*, vol.15, pp. 132-141, Oct 2007.
- [6] J. Ma, L. Lu, Y. Zhan, and X. Zhou, “Hierarchical Segmentation and Identification of Thoracic Vertebra Using Learning-Based Edge Detection and Coarse-to-Fine Deformable Model,” *MIC-CAI*, Part I, LNCS 6361, pp. 19-27, 2010.
- [7] H. Chang, D. Yeung, and Y. Xiong, “Super-resolution through Neighbor Embedding,” *CVPR*, pp. 1167-1183, 2004.
- [8] P. Yan, S. Xu, B. Turkbey, and J. Kruecker, “Discrete Deformable Model Guided by Partial Active Shape Model for TRUS Image Segmentation,” *IEEE T-BME*, vol. 57, pp. 1158-1166, 2010.